Available online at www.sciencedirect.com
SCIENCE DIRECT®
Sensors and Actuators A 114 (2004) 302–311
SENSORS AND ACTUATORS A PHYSICAL
www.elsevier.com/locate/sna

Towards the integration of textile sensors in a wireless monitoring suit

M. Catrysse [a,*], R. Puers [a], C. Hertleer [b], L. Van Langenhove [b], H. van Egmond [c], D. Matthys [c]

[a] *K.U.Leuven, ESAT-MICAS, Kasteelpark Arenberg 10, B-3001 Leuven, Belgium*
[b] *Department of Textiles, Ghent University, Technologiepark 907, B-9052 Zwijnaarde, Belgium*
[c] *Department of Paediatrics and Genetics, Ghent University, UZ Gent, De Pintelaan 185, B-9000 Gent, Belgium*

Received 1 July 2003; received in revised form 19 October 2003; accepted 28 October 2003

Available online 25 January 2004

Abstract

In this paper, we present textile sensors for the equipment of a wireless monitoring suit. The suit is intended for the monitoring of electrocardiogram (ECG) and respiration rate of children in a hospital environment. Special attention is given to the dedicated sensor interface circuits. The sensors, which are entirely fabricated out of textile, are integrated in a prototype belt of the monitoring suit. The complete suit will not contain only the sensors, but also the interface, data handling, storage and transmission electronics. Therefore, distributed, miniaturized circuitry, textile interconnections, a textile antenna and hermetic packaging are developed.

Keywords: Biomedical instrumentation; Cardio-pulmonary function monitoring; Intelligent textiles; Textile sensors

1. Introduction

Recently, ambient intelligence has become a popular concept. It is very likely to be the driving force for consumer electronics in the near future [1]: cars and homes will be equipped with distributed networks of sensing and computing elements, resulting in a user and context aware environment. Wearable electronics and intelligent textiles may become key-elements for ambient intelligence. Recent developments illustrate the promising character of wearable electronics and intelligent textiles [2,3].

In the work presented here, wearable electronics and intelligent textiles are used for a medical application: continuous and long-term monitoring of children in a hospital environment. At present, monitoring, using conventional sensor techniques often cause problems: skin irritation, hampering wires, ... Skin irritation and allergic contact dermatitis have been reported [4], caused both by the adhesive part and the gel used in conventional electrocardiograph electrodes. By integrating sensors, data processing, storage and transmission circuitry in clothing, the patient's comfort, mobility and privacy is increased [5]. Moreover, as textile materials are used for the sensors, antenna and interconnections, the integration is increased, resulting in even more patient-friendliness and the washability (and thus reuse) of the suit is obtained.

Fig. 1 shows a schematic overview of the wearable monitoring unit. Two physiological parameters, respiration rate and ECG, are measured, using dedicated textile sensors: the Respibelt and Textrodes. The measured data is handled in a microprocessor and useful data can be stored in a serial EEPROM. If necessary, an alarm can be activated. An inductive link provides wireless power transmission to the suit, such that the battery can be recharged, and bi-directional data transmission. In this way, the stored data can be retrieved and analyzed on a PC and data processing parameters can be reprogrammed.

2. ECG measurement

2.1. Textrodes

As an alternative for conventional gel electrodes, both woven and knitted stainless steel electrodes, called 'Textrodes' (Fig. 2), are developed for the measurement of ECG. The advantage of the Textrodes is their non-irritating character (in contrast to the gel electrodes) and the possibility of integration in a shirt or suit. The major drawback is the inherent

* Corresponding author. Tel.: +32-16-32-1108; fax: +32-16-32-19-75.
E-mail address: micheal.catrysse@esat.kuleuvan.ac.be (M. Catrysse).

0924-4247/$ – see front matter © 2003 Elsevier B.V. All rights reserved.
doi:10.1016/j.sna.2003.10.071

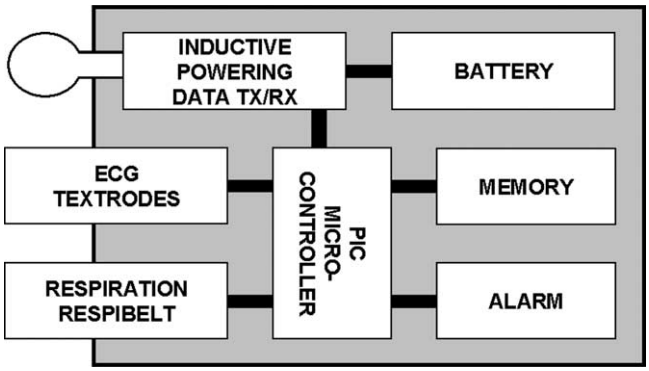

Fig. 1. Schematic overview of the wearable electronics.

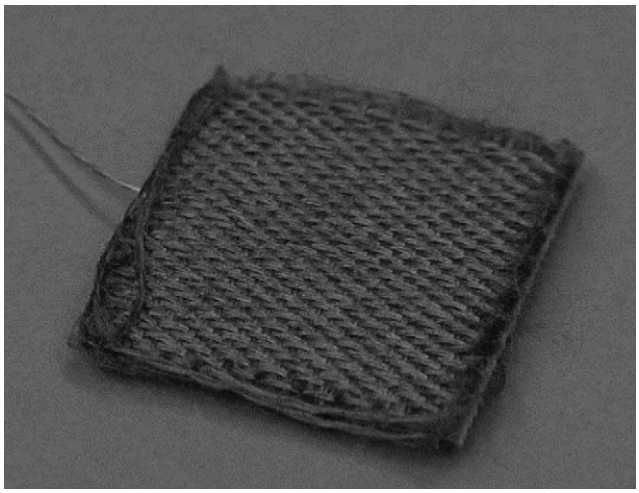

Fig. 2. Photograph of a knitted 3 × 3 cm Textrode.

high skin-electrode impedance. The (dry) skin-electrode impedance of the Textrodes is in the range of 1–5 MΩ cm^2, in the 5–100 Hz frequency range, compared to a typical 10 kΩ cm^2 for commercially available gel electrodes. In Fig. 3, a model for the skin-electrode impedance is depicted. The model consists of the skin impedance Z_{skin}, an dc offset potential $V_{dc\text{-}offset}$, impedance of the conducting gel Z_{gel} (if gel is used) and the electrode impedance $Z_{electrode}$. The conducting gel used in conventional electrodes, partly shortcircuits the skin impedance. The impedances $Z_{electrode}$ and Z_{gel} can be neglected compared to Z_{skin}, as Z_{skin} is much larger than $Z_{electrode}$ and Z_{gel} [6]. This results in a simplified model, consisting of a dc offset potential $V_{dc\text{-}offset}$ and an impedance $Z_{skin\text{-}electrode}$ which is approximated by Z_{skin}. The higher skin-electrode impedance of the Textrodes results in a reduced signal-to-noise ratio (SNR). The main noise sources in ECG measurements are motion artifacts and common mode interference. The noise signal caused by motion artifacts V_{ma} can be adapted from [7] and is approximated by formula (1), assuming $Z_{in} \gg Z_{skin\text{-}electrode}$:

$$V_{ma} = 2\left[\Delta V_{dc\text{-}offset} + \Delta Z_{skin\text{-}electrode}\left(\frac{(V_{ECG}/2) + V_{dc\text{-}offset}}{Z_{in}} + I_{bias}\right)\right] \quad (1)$$

where $\Delta V_{dc\text{-}offset}$ is the variation of the dc-offset of the skin-electrode interface, caused by motion; $\Delta Z_{skin\text{-}electrode}$ is the variation of the skin-electrode interface impedance, caused by motion; Z_{in} is the input impedance of the read-out amplifier; I_{bias} is the bias current of the read-out amplifier.

As can be seen, the motion artifact noise signal consists of two terms, comprised in the model of Fig. 3. In the first place, motion causes a change in the dc-offset of the skin-electrode interface. A second term is the change in skin-electrode interface impedance caused by motion.

Fig. 4 gives a schematic overview of the origin of the common mode interference V_{cm}. The expressions for V_{cm} can be adapted from [8]. For a two electrode configuration (without the third reference electrode) and three electrode configuration, the respective common mode interference V_{cm2} and V_{cm3} are approximated by formula (2) and (3), assuming $Z_{in} \gg Z_{skin\text{-}electrode}$.

$$V_{cm2} = I_d \frac{Z_{in}}{2}\left(\frac{|Z_{skin\text{-}electrode1} - Z_{skin\text{-}electrode2}|}{Z_{in}} + \frac{1}{CMRR_{amplifier}}\right) \quad (2)$$

$$V_{cm3} = I_d Z_3\left(\frac{|Z_{skin\text{-}electrode1} - Z_{skin\text{-}electrode2}|}{Z_{in}} + \frac{1}{CMRR_{amplifier}}\right) \quad (3)$$

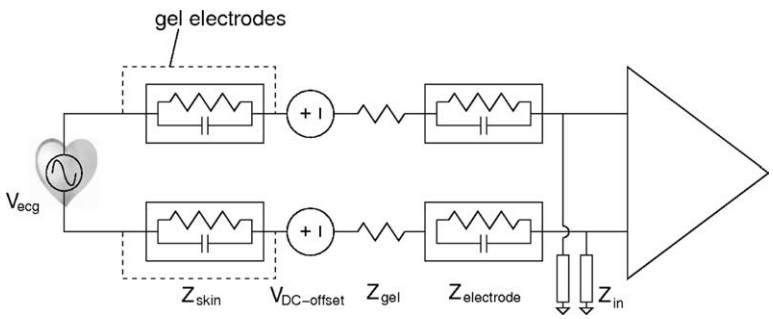

Fig. 3. Model for the skin-electrode impedance and the motion artifacts.

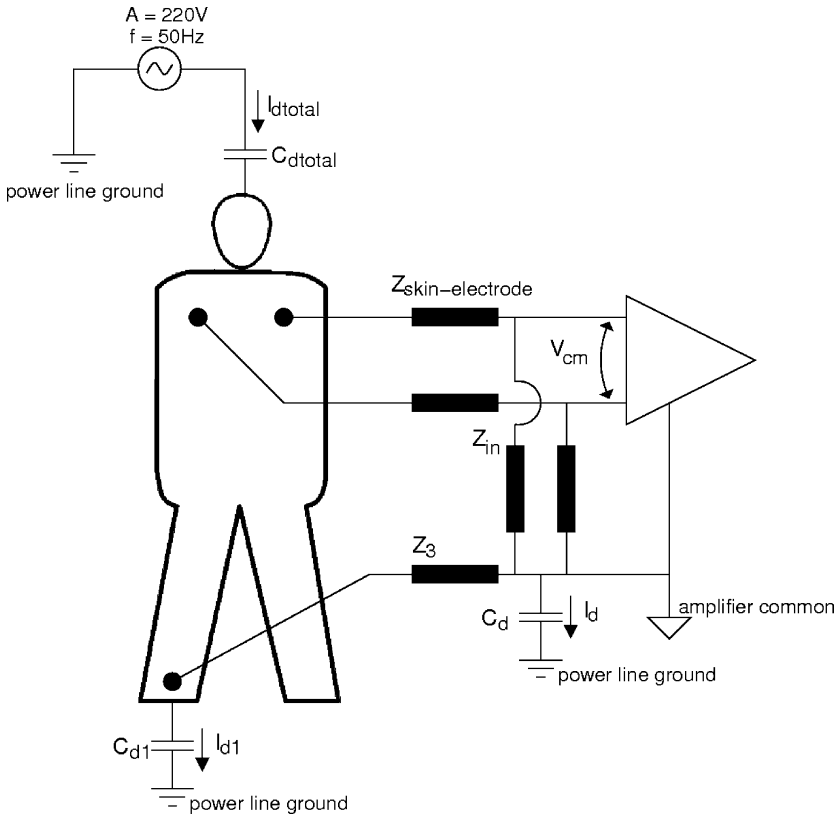

Fig. 4. Model for the common mode interference. Z_3 is used as a ground electrode, but by substituting it's value with formula (6) this model is also valid for a right leg drive circuit.

where $Z_{\text{skin-electrode}}$ is the skin-electrode interface impedance; Z_{in} is the input impedance of the read-out amplifier; I_d is the displacement current in read-out amplifier, caused by common mode; $\text{CMRR}_{\text{amplifier}}$ is the common mode rejection ration of the read-out amplifier; Z_3 is the skin-electrode impedance of the third (reference) electrode.

Typical values for all parameters are given in Table 1. It can easily be seen from formulae (1) through (3) that a three electrode configuration and a read-out amplifier with a high input impedance, a low bias current and a high CMRR are preferred.

2.2. Interface circuit

To overcome the problems associated with this high skin-electrode impedance, the read-out amplifier of Fig. 5 is used. It consists of an instrumentation amplifier, with a bootstrapped input stage and an active right leg drive. The operational amplifier OPA251 (Burr-Brown Texas Instruments) is chosen for its low power consumption, low bias current and high CMRR. The feedforward mechanism of the bootstrapped input stage guarantees a high input impedance [9], which is given by:

$$Z_{\text{in}} \approx R_{\text{bt1}} + R_{\text{bt2}} + j\omega R_{\text{bt1}} R_{\text{bt2}} C_{\text{bt}} \tag{4}$$

This is illustrated in Fig. 6, where the input impedance of the bootstrapped stage is compared to the input impedance of an operational amplifier (OPA251). Following values were selected for the components: $R_{\text{bt1}} = 1\,\text{M}\Omega$; $R_{\text{bt2}} = 1\,\text{M}\Omega$; $C_{\text{bt}} = 1\,\mu\text{F}$.

The instrumentation amplifier converts the differential ECG signal into a single-ended signal, with a high common mode rejection [10]. The CMRR of the complete amplifier equals the CMRR of the instrumentation amplifier and is given by:

$$\text{CMRR} \approx \frac{\text{CMRR}_{\text{OA}}(R_{\text{ia1}} + 2R_{\text{ia2}})}{R_{\text{ia1}}\text{CMRR}_{\text{OA}} + R_{\text{ia1}} + 2R_{\text{ia2}}} \tag{5}$$

where CMRR_{OA} is the CMRR of the operational amplifier.

An active right leg drive is used to reduce the common mode noise [11]. The common mode signal of the two measurement electrodes is averaged by the resistors R_{rld1}, inverted (a 180° phase shift is applied) and fed back to the

Table 1
Typical values for all parameters determining the noise in ECG measurements

	Gel electrodes	Textrodes
$Z_{\text{skin-electrode}}$ at 10 Hz	10 kΩ ± 0.5 kΩ ‖ 140 nF ± 20 nF	2 MΩ ± 100 kΩ ‖ 700 pF ± 100 pF
$\Delta Z_{\text{skin-electrode}}$ at 10 Hz (kΩ)	1	100
$V_{\text{dc-offset}}$ (mV)	15	
$\Delta V_{\text{dc-offset}}$ (mV)	2.5	
I_d (μA)	0.5	
V_{ECG} (mV)	5	

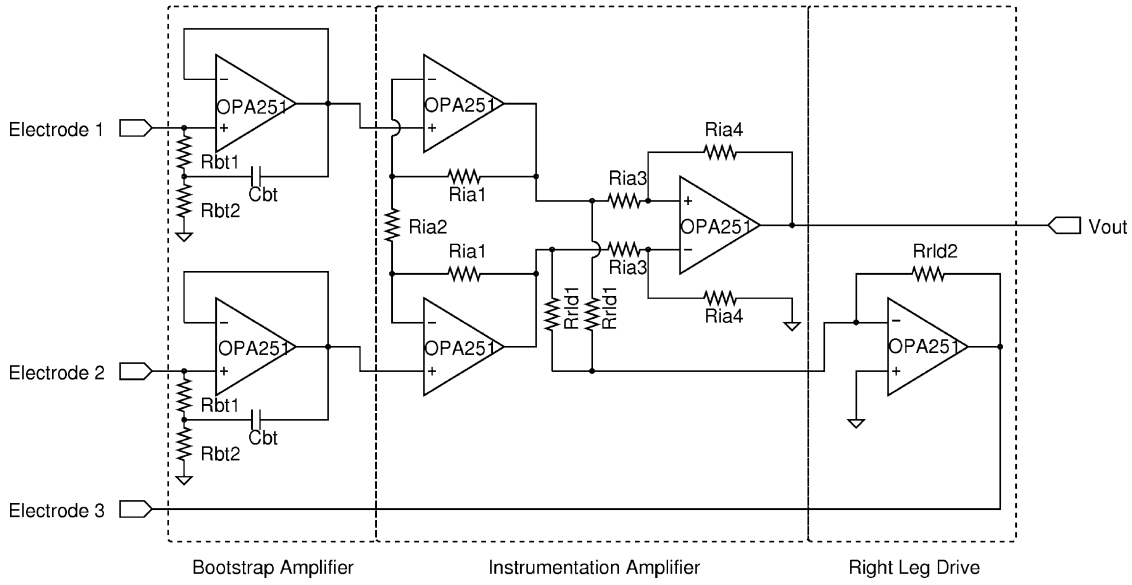

Fig. 5. Schematic overview of the ECG read-out amplifier.

body by the third electrode, in this way annihilating the common mode voltage on the body. Compared to the use of a third electrode connected to the amplifier common, the active right leg drive reduces the skin-electrode interface impedance of the third electrode, as seen by the amplifier, and thus resulting in a lower common mode noise. Z_3 in formula (3) can be replaced by Z_3':

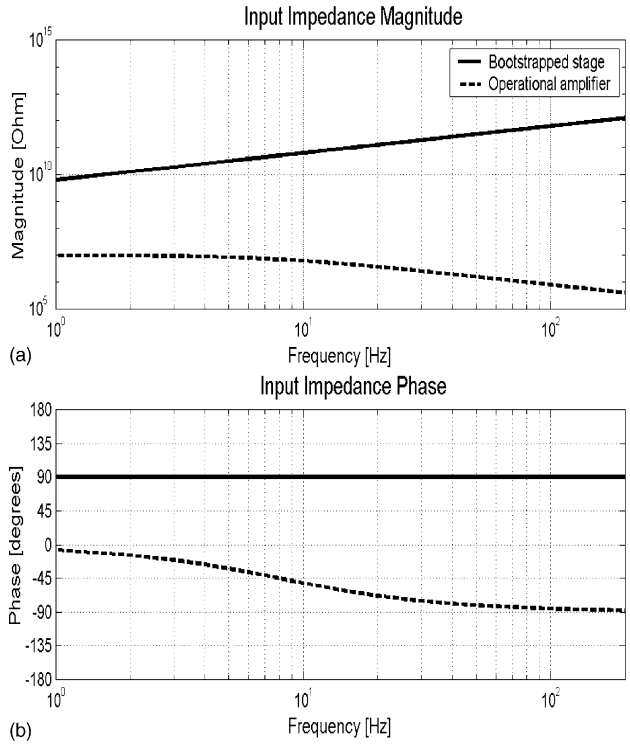

Fig. 6. Input impedance of the bootstrapped input stage compared to the input impedance of an operational amplifier.

Table 2
Specifications of the ECG read-out amplifier

Input impedance at 10 Hz (GΩ)	6.3
CMRR (dB)	85
SNR motion artifacts (dB)	0
SNR common mode interference (dB)	35
Power consumption (mW)	0.96

$$Z_3' = \frac{Z_3}{2R_{\mathrm{rld2}}/R_{\mathrm{rld1}} + 1} \tag{6}$$

The specifications of the read-out circuit are summarized in Table 2. It is clear from Table 2 that by proper amplifier design, it is possible to eliminate the noise caused by common mode interference. Motion artifact noise however, is still dominant. As this is a very low frequency signal, most of the motion artifact noise can be avoided by filtering, having the disadvantage of a partly loss of the ECG signal as well. Some typical ECG measurements are shown in Fig. 7 for both classical electrodes as well as Textrodes. The signals is already filter with a RC band pass filter with cutoff frequencies of 0.5 and 200 Hz.

3. Respiration measurements

3.1. Respibelt

Respiration measurements are commonly carried out in different ways [12,13]: magnetometers measure variation in diameters, strain measure variations in circumference and inductance plethysmography is said to measure cross-sectional area variation. Thorough analysis of inductance plethysmography however [14], demonstrated that this method cannot provide a direct measure of the cross-sectional area,

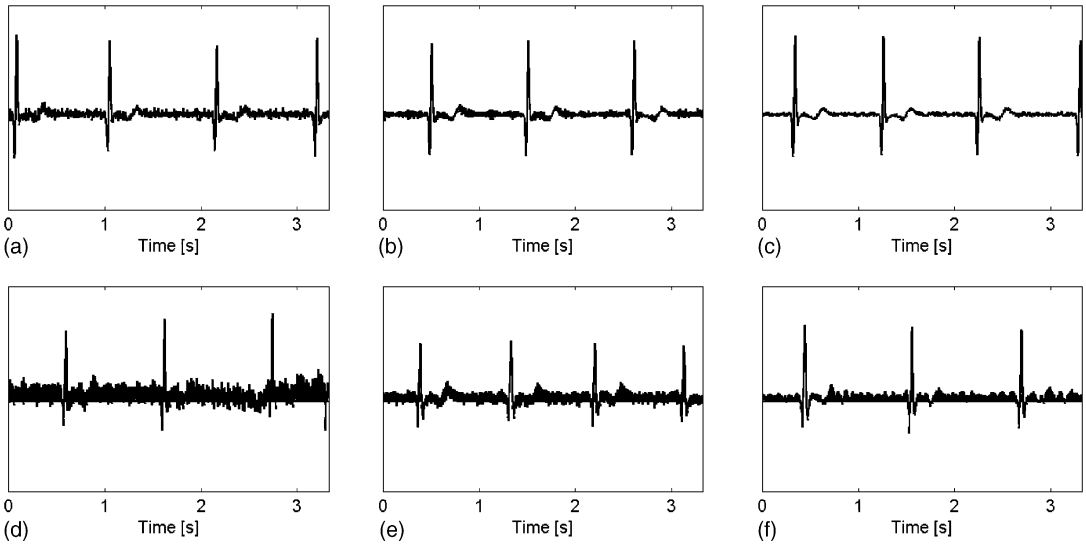

Fig. 7. ECG measurements (a) using gel electrode and circuit from Fig. 2 without active right leg drive and bootstrapped amplifier; (b) using gel electrodes and circuit from Fig. 2 without active right leg drive; (c) using gel electrodes and circuit from Fig. 2; (d) through (f) same as (a) through (c), using Textrodes.

but that the measured inductance variation is a complicated function of the shape and the length of the loop. Most studies reported that, for long term monitoring, when one is only interested in respiration rate, there is no significant difference between the strain gauges measurements and inductance plethysmography.

We present a fabric sensor, called the 'Respibelt', which can replace the conventional respiration measurement methods. The Respibelt is made of a stainless steel yarn, knitted in a Lycra-containing belt, providing an adjustable stretch (Fig. 8). By placing the Respibelt as a coil around the abdomen or thorax, circumference and length changes of the Respibelt, caused by breathing, result both in an inductance and resistance variation. In this way, both changes in perimeter and cross-section are measured. Fig. 9 shows the resistance and inductance variation of the Respibelt as a function of the length. The gauge factor of the resistor is measured to be –0.53. The negative value indicates that stretching the Respibelt results in a resistance decrease. This decrease in resistance is caused by the tightening of the nooses of the knitted structure under stretch. The inductance variation due to stretch of the Respibelt is 0.05 μH/cm. The general expression for the inductance L_{coil} of single turn coil [15], given by formula (7), can be adapted and fitted to the measurement results, taking into account the linear approximation (8) for the relation between the coil diameter D and the wire diameter d. This results in formula (9).

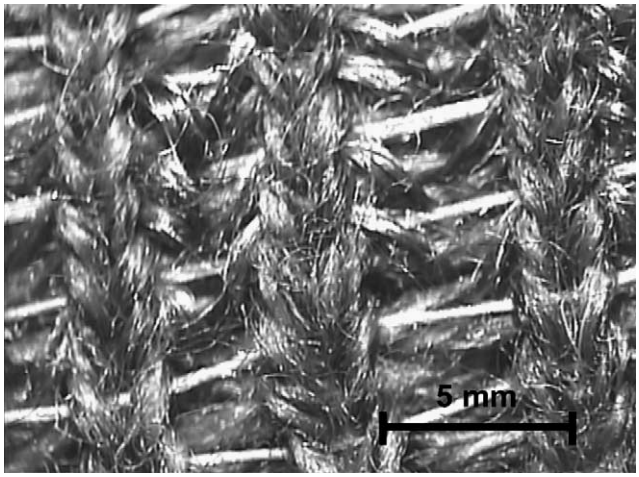

Fig. 8. Detail of the Respibelt respiration sensor.

$$L_{\text{coil}} = 0.0063D\left(2.303\log_{10}\left(\frac{8D}{d}\right) - 2 + \mu\delta\right) \tag{7}$$

$$\frac{8D}{d} \approx \alpha l^2 + \beta l + \gamma \tag{8}$$

$$L_{\text{Respibelt}} = 0.0046l\log_{10}\left(al^2 + bl + c\right) \tag{9}$$

where D is the coil diameter, d the wire diameter, l the coil length, μ the magnetic permeability, δ the skin effect factor and α, β, γ, a, b, c are the fitting parameters.

Next to this empiric approach, the Respibelt structure is simulated using different software packages. Fasthenry [16] is used for the finite element simulation of the Respibelt inductance, whereas Weftknit [17] is used for a qualitative study of the strain gauge effect. The qualitative approach of the Weftknit software gives an explanation for the negative strain gauge (Fig. 10): when stretch is applied to the Respibelt (which is during breathing in), the nooses of the knitting structure tighten. This results in a better conductive contact between the nooses and thus a lower resistance.

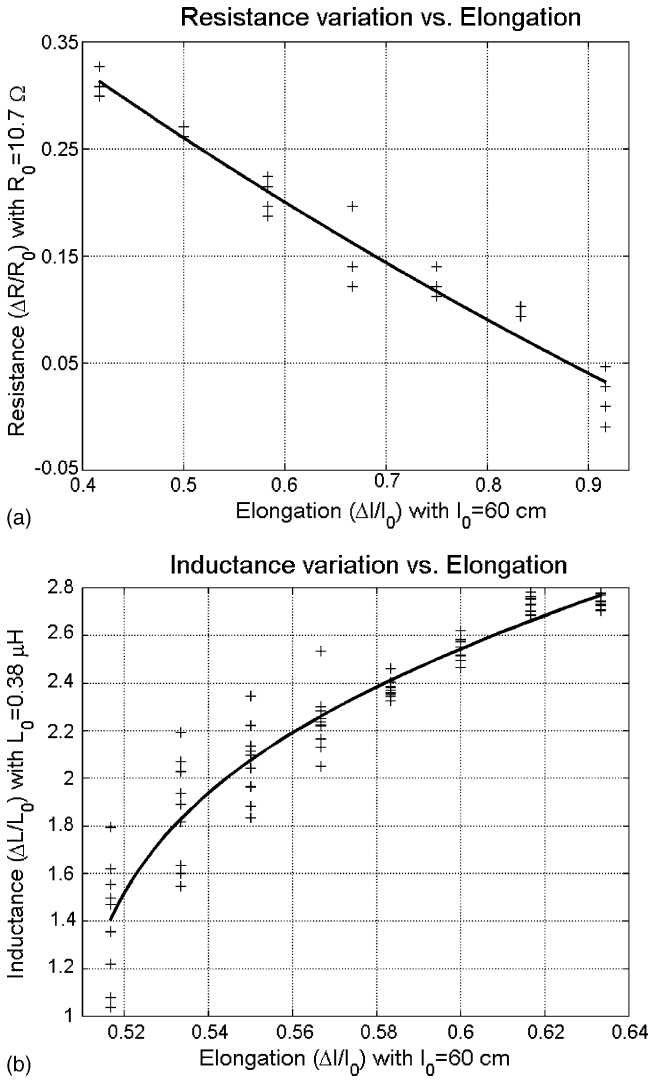

Fig. 9. Resistance and inductance variation of the Respibelt as a function of elongation. The Respibelt rest length l_0 is 60 cm. For respiration measurements, the Respibelt is applied on the abdomen with a pre-strain of 0.5 to avoid the strong non-linearities at low strain levels.

3.2. Interface circuit

To combine these two effects in a single read-out system, the Respibelt is used as a part of an XOR-oscillator of which the resonance frequency depends on both its inductance and resistance (Fig. 10). The reference oscillator (XOR 1) of Fig. 11 is tuned to 2.5 MHz, whereas the measurement

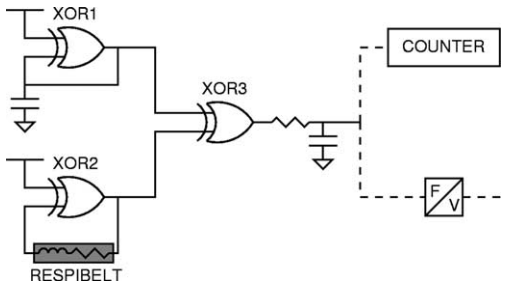

Fig. 11. Read-out circuit for the Respibelt.

oscillator (XO2 & Respibelt) runs at a frequency of approximately 2.2 MHz. The sensitivity of the Respibelt results in 3070 Hz/cm. The measurement signal is downconverted by XOR3 and the filter to a frequency of about 300 kHz. With a circumference variation of about 2 cm due to breathing, the frequency-modulated signal is converted to a digital signal by a counter or an analog signal by a frequency-to-voltage (*F–V*) converter. After demodulation, additional digital or analog filtering is necessary, to eliminate motion artifacts and drift. In Fig. 12, some typical measurement results are depicted. For the demodulation, a counter and an IIR 2nd order Chebychev bandpass filter are used, with cut off frequencies of 0.03 and 0.4 Hz.

4. Wireless power and bi-directional data transmission

To transmit the recorded data from the Textrodes and the Respibelt wirelessly from the suit to a base station, an existing inductive link [18] is adapted and integrated in the suit. The inductive link, consisting of two coils, is able to transmit bi-directional data at a bit rate of 60 kbit/s. Simultaneously, 50 mW can be wirelessly transmitted from the base station to the suit. The primary (base station) coil is integrated in a mattress, the secondary coil is embroidered on the suit. In this way, data can be transmitted and power transferred to the wearable electronics while the patient lies down on his bed. This power transfer ensures continuous operation of the system and can also be used to recharge the battery. Fig. 13 shows the secondary coil. It concerns a 6 turns spiral inductor with a diameter of 12.5 cm, consisting of stainless steel yarn, with an inductance of 2.9 μH and a quality factor of 0.72 at 700 kHz. The inductive link operates within a maximal coil separation range of 6 cm at a frequency of 700 kHz.

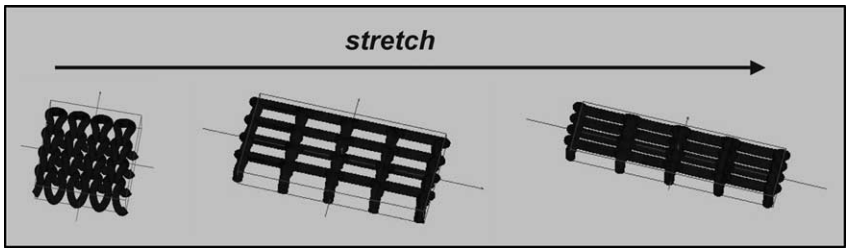

Fig. 10. Weftknit simulation of the Respibelt structure.

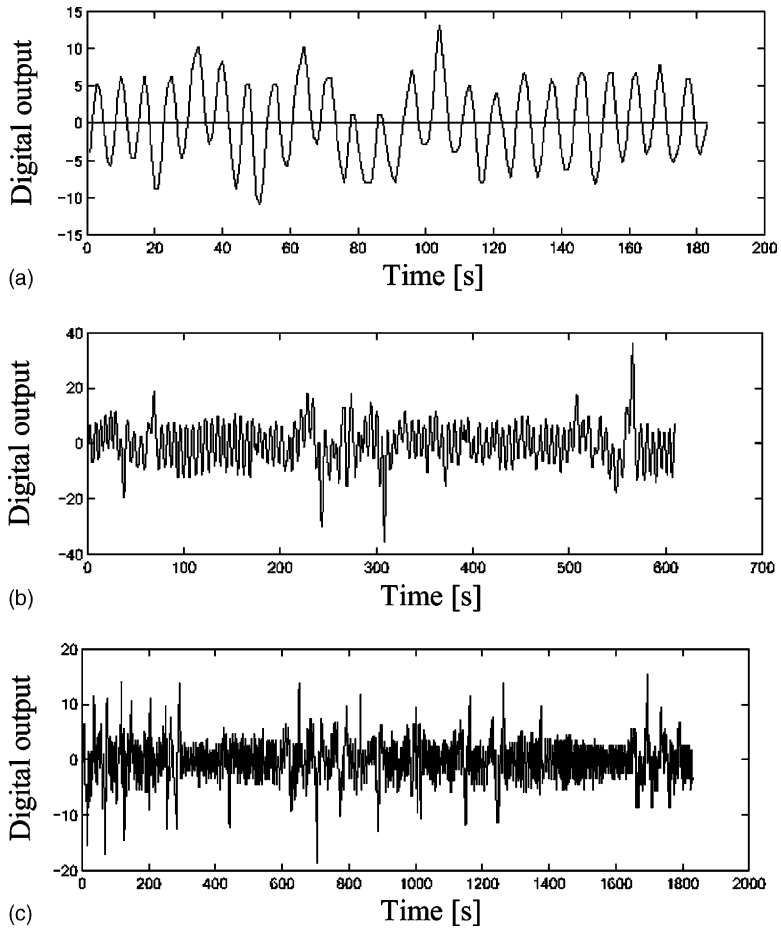

Fig. 12. Respiration measurements with the Respibelt: (a) 3 min measurement; (b) 10 min measurement; (c) 30 min measurements.

Several antennas have already been integrated in clothes for mobile phone communication [19] or Radio Frequency Identification tags (RFID tags) [20,21], but neither of these developments combines the bi-directional data and power transmission, albeit over a short range.

5. Data processing and storage

The data processing and storage unit consists of a PIC16C771 microprocessor (Microchip) and a 24LC64 serial EEPROM (Microchip). In a first phase, a simple peak

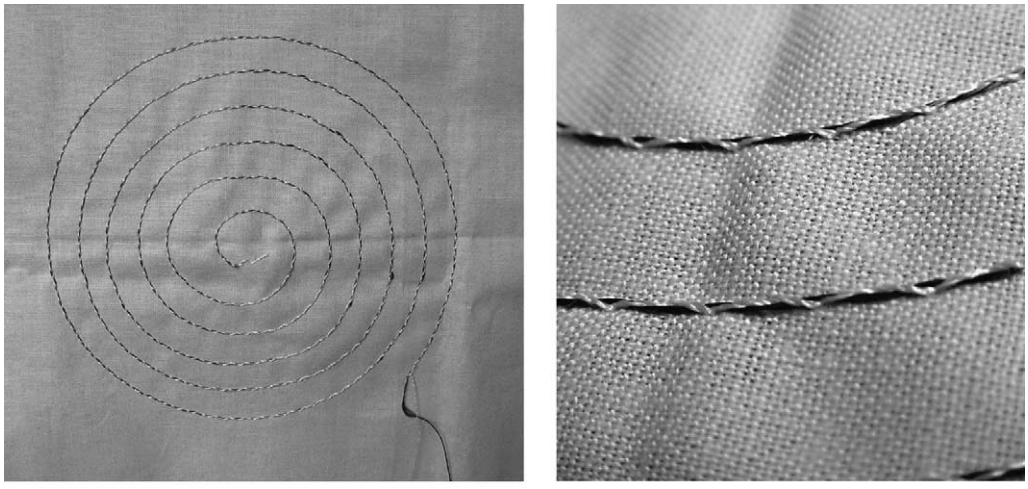

Fig. 13. (a) Embroidered secondary coil of the inductive link. (b) Detail.

Fig. 14. Prototype belt of the intelligent suit.

detection [22] and heart rate calculation algorithm is implemented on the microprocessor for the ECG measurements. For the respiration measurements a counter, additional filtering and a respiration rate calculation algorithm are implemented. Both heart rate and respiration rate are stored in the EEPROM and are easily read out to a PC via the inductive link, making use of the RS232 protocol.

After some clinical experiments, more elaborated functions will be implemented, allowing continuous, long-term monitoring. An event recording function will be used to store only the clinical relevant data. The alarm function will activate a buzzer when a parameter drops below or exceeds a critical value. The exact parameters for theses functions will be decided following the clinical experiments.

6. Integration

The Textrodes and the Respibelt will be integrated in a monitoring suit for children. A prototype belt is shown in Fig. 14. The Textrodes are integrated in the Mickey Mouse ears. The complete suit must not only contain the sensors, but also the sensor interface and data handling, storage and transmission circuitry. Special attention is given to the miniaturization and packaging of the circuitry: comfort and washability of the suit should be preserved.

The circuitry is conceived as a distributed network, integrated in the suit. It is placed on four hybrid boards. On a first board the ECG read-out circuit is placed, the second board contains the respiration read-out circuit, the third one contains the data processing and storage unit and on the fourth board, the wireless link circuit is placed. The boards have a diameter of 2.1 cm and a thickness of 2 mm (Fig. 15). These hybrid boards will be tied as buttons on the suit. For the interconnections between the boards, sensors and antenna, a bus system is currently under development, consisting of stainless steel yarn. This bus system will be integrated in the suit in such a way that it will not hamper the patient.

A hermetic encapsulation will also be developed, providing a washable packaging for the electronics. At present, this is still one of the major challenges to be tackled, not only for this specific project presented here: it remains the bottleneck in every wearable electronics or intelligent textiles development [23].

7. Conclusion

With this work, we demonstrate that textile materials themselves have a strong potential to be used as sensor elements, antennae and interconnections in a wearable bioinstrumentation system. Despite the low quality of the textile sensors, the use of high specifications provides reliable monitoring. Major benefits are the improved patient comfort and the reusability of the sensors. Washable packaging of the electronics remains the major challenge to be tackled, not only for the specific system presented here, but for all wearable electronics and intelligent textiles developments.

(a) (b)

Fig. 15. (a) Concept of the integration: distributed network with stainless steel yarn bus system. (b) Detail of the ECG read-out circuit button.

Acknowledgements

The support of Mr. Pol Speleers (Bekintex, Belgium), Prof. Eric Desoppere (Ghent University) and Prof. Stepan Lomov (K.U.Leuven) is acknowledged. The authors would like to thank the support of the ESAT-MICAS technical staff: Michel De Cooman, Camille Evers and Albert Boon. This research project is supported by the IWT, in the framework of the STWW program, contract no. 000160.

References

[1] F. Boekhorst, Ambient intelligence: the next paradigm for consumer electronics. How will it affect silicon? in: Proceedings of the IEEE ISSCC, San Francisco, USA, February 2002, pp. 28–31.
[2] E.R. Post, M. Orth, P.R. Gershenfeld, N. Russo, E-broidery—Design and fabrication of textile-based computing, IBM Syst. J. 39 (2000) 840–860.
[3] A. Mazzoldi, D. De Rossi, F. Lorussi, E.P. Scilingo, R. Paradiso, Smart textiles for wearable motion capture systems, AUTEX Res. J. 2 (4) (2002) 199–203.
[4] M. Avenel-Audran, A. Goossens, E. Zimmerson, M. Bruze, Contact dermatitis from electrocardiograph-monitoring electrodes: role of *p-tert*-butylphenol-formaldehyde resin, Contact Dermatitis 48 (2003) 108–111.
[5] F.H. Wilhelm, E. Handke, W.T. Roth, Measurement of respiratory and cardiac function by the LifeShirt^{TM}: initial assessment of usability and reliability during ambulatory sleep monitoring, Biol. Psychol. 59 (2002) 250–251.
[6] D.K. Swanson, J.G. Webster, A model for skin-electrode impedance, in: H.A. Miller, D.C. Harrison (Eds.), Biomedical Electrode Technology: Theory and Practice, Academic Press, New York, 1974, pp. 117–128.
[7] P. Zipp, H. Ahrens, A model of bioelectrode motion artefact and reduction of artefact by amplifier input stage design, J. Biomed. Eng. 1 (1979) 273–276.
[8] N.V. Thakor, J.G. Webster, Ground-free ECG recording with two electrodes, IEEE Trans. Biomed. Eng. 27 (12) (1980) 699–704.
[9] R.P. Betts, B.H. Brown, Method for recording electrocardiograms with dry electrodes applied to unprepared skin, Med. Biol. Eng. 13 (1976) 313–315.
[10] J.G. Webster, Medical Instrumentation—Application and Design, Wiley, New York, 1998.
[11] B.B. Winter, J.G. Webster, Driven-right-leg circuit design, IEEE Trans. Biomed. Eng. 30 (1) (1983) 62–66.
[12] G.P. Heldt, Simultaneous Quantification of Chest Wall Distortion by Multiple Methods in Preterm Infants, Am. Rev. Respir. Dis. 138 (1988) 120–125.
[13] R.I. Ross Russel, P.J. Helms, Evaluation of three different techniques used to measure chest wall movements in children, Eur. Respir. J. 7 (1994) 2073–2076.
[14] P. Martinot-Lagarde, R. Sartene, M. Mathieu, G. Durand, What does inductance plethysmography really measure? J. Appl. Physiol. 64 (1988) 1749–1756.
[15] F.E. Terman, Radio Engineers' Handbook, McGraw-Hill, New York, 1943.
[16] M. Kamon, M.J. Tsuk, J. White, FASTHENRY: a multipole-accelerated 3-D inductance extraction program, IEEE Trans. Microwave Theory Techn. 42 (9) (1994) 1750–1758.
[17] S.V. Lomov, I. Verpoest, Modelling of the internal structure and deformability of textile reinforcements WiseTex software, in: Proceedings of European Conference on Composite Materials, Bruges, Belgium, 2002, CD-ROM paper 336.
[18] M. Catrysse, B. Hermans, R. Puers, An inductive powering system with integrated bidirectional datatransmission, Proc. Eurosens. (2003) 843–846.
[19] P.J Massey, Fabric antennas for mobile telephony integrated within clothing, in: Proceedings of the London Communications Symposium, September 2000, http://www.ee.ucl.ac.uk/lcs.
[20] A.P.J. Hum, Fabric area network—a new wireless communications infrastructure to enable ubiquitous networking and sensing on intelligent clothing, Comput. Networks 35 (2001) 391–399.
[21] S. Jung, C. Lauterbach, M. Strasser, W. Weber, Enabling Technologies for disappearing electronics in smart textiles, in: Proceedings of the IEEE ISSCC, San Francisco, USA, February 2003, pp. 386–387.
[22] B.U. Köhler, C. Hennig, R. Orglmeister, The principles of software QRS detection, IEEE Eng. Med. Biol. 21 (1) (2002) 42–57.
[23] P. Lukowicz, G. Tröster, Packaging issues in wearable computing, in: Proceedings of the International Workshop on Chip Package Codesign, Zurich, Switzerland, March 2000, pp. 19–22.

Biographies

M. Catrysse was born in Brugge, Belgium, in 1975. He received his M.S. degree in Microelectronics from the K.U. Leuven in 1998. In 1998, he joined the ESAT-MICAS laboratory at the K.U. Leuven as a research assistant. He is currently working towards a Ph.D. His main research interests are inductive powering and low power data transmission for biomedical applications, smart medical implants and intelligent textiles.

R. Puers was born in Antwerpen, Belgium in 1953. He received his B.S. degree in electrical engineering in Ghent in 1974 and his M.S. degree at the Katholieke Universiteit Leuven in 1977, where he received his Ph.D. degree in 1986. He is currently Professor at the Katholieke Universiteit Leuven, Belgium and Director of the Clean Room Facilities for Silicon and Hybrid Circuit Technology at the ESAT-MICAS Laboratories of the same University. He teaches courses of "microsystems and sensors", "biomedical instrumentation and stimulation", "technology for hospitals" and "electronics, automatization and IT". His main research interests are: biomedical implant systems (monitoring and stimulation); transducer and actuator principles; mechanical sensors (pressure, accelerometers, strain gauges, temperature, etc.), silicon micromachining; packaging an interconnection techniques (hybrids, hermetic and biocompatible sealing, etc.) and biotelemetry (inductive power delivery, bi-directional data communication). Prof. Puers is involved in the organization, reviewing and publishing activities of many conferences, journals and workshops in the field of biotelemetry, sensors, actuators, micromachining and microsystems. He is the author of more then 220 papers on biotelemetry, sensors or packaging in journals or international conferences.

C. Hertleer graduated as a Master of Science in Textiles in 1990 at the Ghent University in Belgium, Department of Textiles. For three years, she worked in a vertically integrated textile company that produces terry cloth. She worked during 6 years in a bank office but in June 2000, she decided to return to her roots: textiles. Since then, she works as a researcher at the textile department of the University where she studied. She gives classes in Weaving and Jacquardtechnology, but her activities are mainly concentrated on intelligent textiles, more specifically the research and development of textile sensors.

L. Van Langenhove was born in 1961. She graduated as a textile engineer at the University of Ghent in 1984. From 1984 until 1989 she worked as a assistant research manager at UCO (integrated textile mill: spinning, weaving, dyeing and finishing, printing, geotextiles). Her tasks were: research in spinning, external research projects in all areas. From 1989 until today, she works at the Department of Textiles, University of Gent, were she obtained a Ph.D. on yarn modelling in 1994. Since 1997 she is a professor. The research group that she is leading has its activities in

technical improvements on air jet looms, simulation of weft insertion on air jet and rapier looms, applications of spider silk in tissue engineering, development of textile sensors for medical applications and biomemetics in textiles. The department is further involved in several European Educational Textile Projects. Lieva van Langenhove is author or co-author of more than 60 papers in international journals and papers at international conferences.

D. Matthys was born in Ghent, Belgium in 1951. He finished medical school in 1974 (Ghent University). He trained in pediatrics at the University Hospital of Ghent (1974–1979) and in pediatric cardiology (University Hospital Ghent and London, Hospital for Sick Children, Great Ormond Street). He obtained a Ph.D. in 1999 at Ghent, University. He is currently Professor in Pediatrics at Ghent University and head of the department of Pediatrics at Ghent, University Hospital.